FINAL REPORT

A PRELIMINARY STUDY OF A CRYOGENIC EQUIVALENCE PRINCIPLE EXPERIMENT ON SHUTTLE

NAS8-33796

Principal Investigator: C. W. F. Everitt

Associate Investigator: Paul W. Worden, Jr.

W. W. Hansen Laboratories of Physics
Stanford University
Stanford, CA 94305

January 8, 1985

different accelerations and tend to follow different orbits. This shows up as a differential force between them which has the same period as the orbit.

The proposed experiment is operated at cryogenic temperature. The two masses are supported in superconducting magnetic bearings and have their positions measured by superconducting position detectors. The chief advantages of cryogenic operation are essentially perfect shielding from electromagnetic disturbances, extreme mechanical and thermal stability, virtual elimination of radiation pressure, and the possibility of working in a much higher vacuum. The reduction in thermal noise which is commonly cited as a big advantage of cryogenic operation is an insignificant factor in this experiment.

The masses are supported in independent magnetic bearings which are very stiff radially and almost force-free along the cylinder axis. This configuration is chosen to allow precise centering of the masses on one another. If the masses have their centers of mass at the same position, gravity gradient forces which might mimic a violation of the equivalence principle are minimized. This mass centering is possible with separate concentric cylinders, but not for rigidly joined masses in a torsion balance; and concentric spheres have the problem of access to the central one. The position detectors observe differences in linear displacement along the common axis of the bearings. Figure 2 shows the arrangement for the present version of the Earth-based laboratory apparatus.

The chief advantage of operating in space is that the magnitude of the effect to be measured is about three orders of magnitude greater than it has been in recent Earth-based experiments, since the driving acceleration is the gravitational attraction of the Earth (about 780 cm/sec^2 at 300 nautical miles altitude) rather than the attraction of the Sun (about 0.5 cm/sec^2). It is also advantageous to have the period of the acceleration about 100 minutes rather than 24 hours, both for convenience and for any potential reduction in 1/f noise. Vibrational or mechanical disturbance to the apparatus is also potentially much less in orbit than on the ground, at least in a carefully designed drag-free satellite. However, this is not true of Shuttle; its acceleration environment is typically ten times worse than the Earth's surface. Thus the expected advantage of a Shuttle-borne version of the experiment relative to the same experiment performed on Earth is only about a factor of 100.

We measure the linear displacement of two freely falling bodies instead of an angular measurement on a torsion balance because of gravity gradient effects. Any torsion balance, however carefully made, has some residual quadrupole mass moment, which will cause a torque in a gravity gradient field. In an experiment at the 10^{-11} level on Earth, the gravity gradients from nearby masses are an annoyance. At the level of 10^{-15}, whether orbital or Earth-based, control of these disturbances is crucial. It is impractical to manufacture a torsion balance to the required accuracy for a 10^{-15} orbital experiment because the Earth's gravity gradient is so large. This difficulty can be eliminated in an experiment with free masses by making the mass-centers of the two bodies coincide. If they do not, there will be a differential acceleration between them which is proportional to the gravity gradient times the displacement. Since the gravity gradient is known and is at the second harmonic of the orbital frequency, its effect can be measured independently of violations of the equivalence principle and the center of mass offset can be calculated from the measurement. The offset can then be controlled with

a servo loop. By this centering operation, one not only eliminates the gravity gradient accelerations from the Earth, but also makes the apparatus insensitive in first order to gravity disturbances from the surrounding spacecraft.

III. Progress Under This Contract

During the funded period we have made significant advances toward a preliminary design for the experiment. Provided that the vibrational noise environment of Shuttle can be overcome as described below, equivalence principle experiments approaching the 10^{-15} level of sensitivity may be possible on Shuttle. We will now describe results in the four categories of work described in section I.

1. Shuttle environment studies.

Mostly during the period 1980 through 1982, we investigated the environment of Shuttle both with regard to possible interference with the experiment and to interfacing with the apparatus. The results were illuminating.

Shuttle would interfere with the experiment principally through its vibrational noise, which is (broadly speaking) typically ten times that of the Earth's surface, although with a rather different frequency spectrum. There are two serious problems. First, high frequency noise is caused by thruster firings and crew motions [2]. This noise would be frequency converted by small nonlinearities in response, and strongly interfere with the test masses in the equivalence principle experiment. Second, low frequency noise is caused by atmospheric drag and solar pressure on the Shuttle, which might have an amplitude of 10^{-8} g in an orbit at 300 nautical miles. Assuming the experiment has the expected common mode noise rejection ratio of 10^5, this alone would limit the measurement to one part in 10^{12}.

Both of these problems can be solved by the notion of isolating the experiment from Shuttle by operating in what we have called a "semi-drag-free" mode. The idea is to have the experiment package free to move inside its helium dewar, over a range of, say, 10 cm. When the package drifts close to contact, Shuttle thrusters are used to prevent contact. Thus the experiment does not feel any thrust or drag on Shuttle or any vibrational noise. Thruster firings would be required about every 10 minutes, consistent with ordinary attitude firings. The semi-drag-free mode would be required for the duration of the experiment, which might be a few orbits. In this mode, gravity gradients from the Shuttle, including crew motions, would probably be the limitation on experimental performance. These effects are summarized in section III.2 below.

We also investigated problems of interfacing with the Shuttle. Because of the requirement for a microgravity environment, the experiment should be located near or at the center of mass of Shuttle. Its power and data requirements are expected to be modest, and we estimate it would need a cylindrical dewar about two feet in diamter and six feet long.

We investigated two alternatives to actually performing the experiment on Shuttle. These were the SPAS (Shuttle PAllett Satellite) and TMS (Teleoperator Maneuvering System). Neither of these systems is designed to be drag-free or have a particularly low vibrational environment, and they would

have to be used in a semi-drag-free mode like Shuttle. The major advantage would be for longer missions without interfering with other experiments.

On the advice of reviewers of the original proposal, we studied alternative room-temperature approaches to a cryogenic orbital equivalence principle experiment. These might use laser or microwave position detectors in place of cryogenic position detectors. A Hewlett-Packard laser interferometer would have adequate sensitivity to use in a 10^{-15} experiment, for example. However, there are serious difficulties with radiation pressure and magnetic forces, even though the forces from a laser beam might be accuragely balanced out. From the discussion in section 3.c below, at room temperature the thermal radiation forces from a temperature gradient across the experimental chamber are far from negligible. A 0.1 millikelvin difference would limit a room-temperature experiment to a one part in 10^{12} measurement. Forces from the magnetic fields of Earth or the Shuttle occur if the test masses are slightly dia- or para-magnetic. An example is the DISCOS drag-free proof mass for the TRIAD I satellite, launched in July 1972 by our colleagues in the Stanford Department of Aeronautics and Astronautics. This used a special gold-aluminum alloy in which the diamagnetic and paramagnetic contributions cancelled to reduce disturbances below 10^{-12}g . This freedom of choice of materials does not exist in an equivalence principle experiment. Superconducting shielding, however, eliminates the problem.

2. Numerical simulations and analysis.

We did several computer simulations of an idealized Shuttle-borne equivalence principle experiment lasting up to one orbit. The intent of these simulations was to study the dynamics of the system of interacting masses comprising the experiment, and the effect of mass interactions and noise on the sensitivity. This was a profitable exercise since we found at least one unexpected problem due to gravity gradients. Analytic solutions confirmed the problem and showed how to control it. The result of the simulations and analysis were 1) that the experiment can be done to one part in 10^{13} in a few minutes, but to achieve one part in 10^{15} requires at least several orbits and possibly several days depending on noise; and 2) in order to do the experiment on Shuttle, the apparatus must be very carefully isolated from vibration and some sort of minimal drag-free control is needed to prevent interference with the measurement.

Figures 3.a and 3.b are typical of the simulated mass motions in response to Shuttle vibration. This particular simulation used a fairly unrealistic noise amplitude and spectrum, and the masses were not controlled except by passive restraints from the magnetic bearings. Other simulations and studies showed the importance of controlling not only the axial positions of the test masses, but also the radial positions. Figure 4 is an example in which the mass positions are uncontrolled. In the section shown, the differential acceleration is about 10^{-13}g (corresponding to a sensitivity of about one part in 10^{13}) due to gravity gradients acting on the center of mass separation. Over one orbit these masses drifted apart about two centimeters and about 30 centimeters relative to a drag-free Shuttle. Controlling the test mass positions reduces the errors to the round-off accuracy of the program.

One unexpected result came from the interaction between displacements at right angles to the bearing axis and gravity gradients. We have expected that this would be negligible with the bearings much stiffer than the negative

spring constant of the gravity gradient. If the constraint forces from a magnetic bearing fixed in the orbiting frame are C_{ij}, the acceleration of a test body of mass M is

$$X = -C_{xx} \cdot \left(\frac{X}{M}\right)$$

$$Y = -C_{yy} \cdot \left(\frac{Y}{M}\right)$$

$$Z = -\left(\omega_o^2 + 3\omega_o^2 \cos^2(\omega_o T) + \frac{C_{zz}}{M}\right) \cdot Z$$

$$-\left(3\omega_o^2 \cos(\omega_o T) \sin(\omega_o T) + \frac{C_{zy}}{M}\right) \cdot Y$$

$$- C_{zx} \cdot \left(\frac{X}{M}\right)$$

where T is the time and ω_o is the frequency of the orbit. Because C_{xx} and C_{yy} are much greater than the gravity gradients and other C_{ij}'s, they dominate the motion in the xy plane, and thus in the steady state X=Xo and Y=Yo; this represents the alignment errors of the bearings with the centers of mass. The terms C_{zi} in the last equation are much smaller than C_{xx} and C_{yy}, but are still of the same order as the gravitational terms and are of unknown size. The C_{zx} term is constant and causes no problems; however, because of the other terms, a difficulty arises when we try to center the masses. The idea was to measure the acceleration, immediately calculate the center of mass displacement which caused it (from the known gravity gradient) and use the result to drive a centering servo. The extra unknown forces from the bearings mean a more complicated mathematical procedure is required which uses the time dependence of the gravitational forces to separate them from the constraint forces. The constraint forces can then be modelled and their effects removed from the centering procedure. Another, better, method is to control Xo and Yo by a modification to the magnetic bearings, and perhaps set additional performance requirements on the bearings as well. For a 10^{-15} experiment, Xo and Yo should conservatively be less than 50 Angstroms, which would guarantee that the amplitude of the doubly periodic gravity gradient force be less than the expected signal from a violation of equivalence. In a low-vibration environment, using position detectors with an intrinsic resolution of 0.01 Å, this is not a difficult requirement, but it does add to the complication of the experiment.

There are several other effects of potential significance. If the orbit is slightly elliptical, there is a subharmonic of the gravity gradient term of order $\varepsilon g \delta R$ where ε is the eccentricity, g the acceleration of gravity, and δR the displacement of the centers of mass. With δR set by the above requirement, $\varepsilon = 0.1$ would not cause a problem; alternatively, if this were the only source of noise at orbital period, the requirement on δR could be relaxed to, say, 5000 Å if $\varepsilon < 0.01$, which is easy to achieve.

A second effect occurs if the common axis of the cylinders is inclined at an angle α to the orbit plane. The free orbits of the test masses may then become inclined to each other: an effect which is equivalent to a singly periodic differential motion of the masses. If the masses are separated by a distance δZ (corresponding to the deadband of the Z-axis controller), the resulting acceleration has magnitude $g\delta Z \sin(\alpha)/R$, and for a 10^{-15} experiment

δZ should not exceed 100 Angstroms. This is automatically achieved if the masses are centered well enough to reduce the gravity gradient acceleration to the required level.

3. Error analysis.

In addition to the simulation studies, we performed some error analysis which is more hardware-related. This included the effects of thermal distortion on the apparatus; gas pressure effects; thermal radiation; and an analysis of the superconducting position detection and differencing system.

a. Thermal distortion effects.

To make a satisfactory differential measurement, the test mass support structure (magnetic bearing and surroundings) must be extremely stable in all dimensions. There are two distinct effects: 1) Even if the structure is perfect at one temperature T, thermal expansion differences between the various parts - and even across one part - will generally make it imperfect at any other temperature $T+\Delta T$; 2) A heat pulse applied locally to the apparatus will make the heated volume expand and cause a transient distortion that lasts until thermal equilibrium is re-established. These distortions affect the apparatus in several ways: they may couple extra forces from the magnetic bearings into the sensitive axial direction; they may distort the position detector structure and cause zero shifts and drift in the position measurement; by changing the size of the inductances in the position detector they will change its sensitivity and offset; and similar changes in the magnetic bearing can change the radial forces on the test mass.

Of the two basic effects, the thermal expansion differences are most important to the Earth-based experiment and the transient distortions from non-equilibrium temperature distributions are most important for the orbital experiment. We will discuss the Earth-based transient distortion problem first, as it can be easily translated into a corresponding effect in the orbital experiment. If α is the thermal expansion coefficient, ΔT the temperature difference between the ends of the bearing, L a characteristic length for the bearings, and h the length of the radial supports connecting the inner and outer bearings, then the change in angle caused by ΔT is

$$\delta\theta = h\alpha\Delta T/L.$$

Note that what counts is the amplitude of the component of the Fourier transform at the signal frequency and that this distortion comes only from an asymmetric temperature distribution. We now analyze the distortion of the central assembly on the assumption that one end is thermally isolated while the other is heat-sunk to a varying temperature; this causes this temperature distribution by changing while the temperature of the structure lags. This is very much a worst-case analysis since in real life both ends are more or less equally heat-sunk.

Let the temperature variation of the heat source be $Te^{i\omega t}$. The relaxation time τ of the structure is

$$\tau = Cv\rho\, L^2/2\kappa$$

where Cv is the specific heat, κ the thermal conductivity and ρ the density of the material. Treating the response of the structure as a first-order system, the temperature difference ΔT caused by the variation of amplitude $\mathbb{T}$ at frequency ω is

$$\Delta T = \mathbb{T} \frac{\omega\tau}{1 + i\omega\tau}$$

which may be combined with the equation for the angle change to get an allowable variation in bath temperature,

$$\mathbb{T} = \frac{2\kappa\delta\theta}{h\alpha\, Cv\rho\, L\omega} = \frac{2\theta\mu}{hL\omega} .$$

Thus $\mu = \kappa/\alpha\, Cv\rho$ is a figure of merit characterizing the material for thermal distortions of this kind. Typical values of μ are 4.8×10^{11} cm^2 °K/sec for sintered alumina, 4.04×10^{13} for fused quartz, 1.05×10^{14} for crystalline sapphire, and 6.5×10^{16} for diamond.

The difference in angle is crucial for the Earth-based experiment, because of the Earth's gravity. The difference in angle $\delta\theta$ causes a relative acceleration $g\delta\theta$ between the test masses which looks exactly like a violation of the equivalence principle. Thus for sensitivity to one part in 10^{13}, we need $\delta\theta$ to be 10^{-16} radian or less. Even so, transient temperature distortions do not necessarily cause problems because of the low signal frequency. For a sintered alumina structure with $L = 15$ cm, $h = 1$ cm, the allowable daily temperature variation is about 0.1 °K.

Much more serious for the Earth-based experiment are angle changes due to different materials used in construction. Clearly, if the apparatus is made of a single homogeneous material, a uniform temperature difference will cause no change in angle: the apparatus simply changes size. The problem is that the apparatus is not made of a single material, and there are differences in expansion between its parts. These cause an angle change $\delta\alpha\Delta Th/L$ where $\delta\alpha$ is the maximum difference in thermal expansion. With $\delta\alpha = 10^{-8}$ per degree (appropriate for the present materials), the temperature amplitude at daily period should be less than a microKelvin in a 10^{-13} Earth-based experiment. This is within the capabilities of cryogenic temperature controllers.

The situation is rather different in the orbiting experiment. External non-gravitational accelerations are the analogy to the effect of the Earth's gravity field on the Earth-based experiment, with the important difference that the residual accelerations in orbit are quite variable and tend to recur at orbital frequency. Thus static angular offsets between the bearing axes are much more important than the changes due to thermal distortions. The alignment of the axes of the bearings for the two test masses is, in fact, one of the stronger reasons for making the experiment as nearly drag-free as possible. If the axes of the inner and outer bearings are misaligned by a small angle Θ, the external acceleration a will couple into the differential motion of the masses by an amount $a\Theta$, which must be less than the acceleration sensitivity of the experiment (10^{-15}g). With an acceleration environment due entirely to drag of 10^{-8}g, Θ needs to be less than 0.02 arc-second - a very difficult alignment to achieve. If non-gravitational accelerations are reduced to 10^{-10} g, Θ needs to be less than 2 arc-seconds, which can be achieved with ordinary differential screw adjustments and some care. A fully drag-free system might achieve 10^{-12} g.

Thermal distortions do have some effect on the orbital experiment. For a 10^{-7} g external acceleration, $\delta\theta$ could be allowed to be as large as 10^{-8} radian in an experiment to one part in 10^{13}. The distortion caused by periodic heating is negligible compared to this. The significant transient effect is caused by variable taper of the bearings. Because the test mass is pressed from all sides by the bearing, a slightly conical bearing tends to expel the mass from one end. An axial temperature gradient will cause a change in cone angle and thus a change in the force on a test mass. The effect may be estimated by using the bearing preload (the acceleration which the test mass would have if half of the bearing were removed) in place of the external acceleration, and the radius r of the bearing in place of h in the above analysis. $\delta\theta$ now becomes the cone angle, and the apparatus is expected to be approximately five times larger in linear dimensions. With a preload of 10^{-3}g, $\delta\theta$ can be allowed to change by as much as 10^{-14} radians, which is possible if the temperature changes less than about 25 milliKelvin at orbital frequency. This regulation is easily achieved.

The considerations regarding the mechanical stability of the position detector coils are very similar to those for distortions of the central bearing assembly. Once again, a uniform change in temperature of the assembly will have little effect if the supporting material for the coils is homogeneous. At 4 °K, the expansion coefficient of alumina ceramic is 3×10^{-11}. A one milliKelvin temperature change would cause an overall change in length of a 15 cm system of 5×10^{-5} Angstroms, which is much smaller than the sensitivity needed to do the experiment. Changes in scale factor are proportional to inductance changes which are in turn proportional to changes in linear dimension; these effects are also small.

b. Gas pressure effects.

The presence of gas in the experimental chamber disturbs the experiment in several ways. First, it adds damping, and therefore contributes to the limit on the experiment from thermal noise. This is not a practical limitation at the accuracy we propose, but is the fundamental limit. Second, a gas pressure gradient, as from outgassing, directly accelerates a mass by exerting different forces on its two ends. Third, a temperature gradient in the presence of gas will accelerate the mass through the radiometer effect, and fourth, residual gas couples the masses to motions of the bearings by viscosity.

Suppose that an area A on one end of a test mass is outgassing at an equivalent pressure P, and that the other end is not outgassing. The pressure will exert a force PA on the body, resulting in an acceleration PA/M, where M is the body's mass. This acceleration should be less than the sensitivity of the experiment ηg where η is the level of equivalence principle sensitivity sought and g is the acceleration at the orbit. This gives a condition on the pressure which is best written in terms of the density ρ and the length l of the test mass:

$$P < \rho g l \eta .$$

For a lead mass 5 cm long, the pressure difference should be less than 3×10^{-14} torr to do a 10^{-13} experiment. This is, however, an extremely conservative requirement, because what counts is not the steady gas streaming force, but the much smaller component of this (or other gas-related disturbances) at orbital frequency which acts like a signal. If the pressure

difference is decreasing exponentially with time constant γ, its amplitude at frequency ω is roughly proportional to $\omega/(\gamma^2+\omega^2)S$ where S is the observation time. This implies that a periodic signal can always be resolved from an exponentially decaying signal if the decay is slow enough or if it is observed long enough. The maximum pressure difference above is multiplied by $(\gamma^2+\omega^2)S/\omega$. The decay constant for outgassing in the disturbance compensation (drag-free) system for the NOVA-1 spacecraft [3] (which was seriously affected by outgassing forces from lexan end plates at room temperature) was 52 days, or about 4.5×10^6 seconds. A similar time constant in the equivalence principle measurement would allow a pressure difference 7×10^5 times greater, or about 2×10^{-8} torr, in a measurement lasting one orbit. This is well within the range of vacuum technology even at room temperature. Recently J. P. Turneaure of Stanford has demonstrated a "low-temperature bake-out" technique which readily gives pressures as low as 10^{-12} torr, a factor of 10^6 lower than the operating pressures used by Roll, Krotkov and Dicke.

The other gas disturbances are intrinsically smaller but may have different time dependencies. The radiometer effect is found by multiplying the conservative pressure estimate by $T/(l dT/dx)$ where l is a characteristic length (of the mass, say) and dT/dx is the temperature gradient. With temperature differences of 10^{-4} K in the test chamber, which are easy to achieve, the conservative estimate for the required pressure is 10^{-11} torr. Any temperature differences would probably tend to change near orbital frequency because of changing heat load from the sun, and so some care should be taken with this. The disturbance from gas coupling is found by multiplying the conservative pressure by Vs/Vo where Vs is the molecular velocity and Vo is the velocity difference between the test mass and bearing. Vs/Vo is of the order of 10^4 for the maximum velocity differences expected near orbital period, so this disturbance is somewhat smaller than the others.

c. Thermal radiation.

Thermal radiation pressure may affect the experiment if there is a temperature difference across the experimental chamber. If opposite sides of a chamber of length l differ in temperature by δT, the masses M are accelerated by radiation pressure by roughly

$$a = 8\sigma T^3 \frac{\delta T A}{3Mc}$$

where A is an effective area for the mass, c is the speed of light, σ is the radiation constant, and T is the temperature. This can be used to set an upper limit on the temperature differences in the chamber.

$$\delta T < 3\eta \frac{gMc}{8\sigma A T^3}$$

where η and g have the same meanings as above. Near room temperature, for a 1 Kg test mass with area 20 cm^2, δT should be less than 0.3 milliKelvin to do a 10^{-15} experiment. This is fairly difficult in view of the vacuum environment and solar thermal heat loads, and would require some sort of dewar structure. At 4 K, the effect of radiation pressure is negligible even for ten degrees across the chamber.

d. Position detector analysis.

As a result of measurements made with the laboratory apparatus, we found it desirable to significantly change the way in which the position detector is used. Originally the concept was to use the position detector as a passive device which could measure the position of the test masses without much affecting their motion. The mass positions were to be controlled by a separate set of control coils placed beneath the test masses. These coils were to be used with a room temperature control circuit to apply small corrections to the mass positions.

In the first concept, the magnetometers were to measure the mass position which would be used as an error signal to an analog control circuit. The analog controller produced currents which were sent to the control coils, and the differential measurement was made by subtracting these currents (interpreted as control efforts) in a precision resistor at room temperature. We succeeded in making this work in an unsatisfactory way before the start of this contract; the problems were with dynamic range and transient response. In order to have the required sensitivity, the SQUID magnetometers had to be used at a fairly high gain; but at this gain, sensmic noise often saturated the magnetometers, either causing them to lose lock or reset to zero according to their preset mode of operation. This saturation generally caused the controller/test mass/magnetometer system to oscillate or perform other undesirable actions. This problem was solved by generating the control law in the computer instead of in the analog circuit, and operating the magnetometers in a flux-counting mode. The history of this system is described in section 4 below. Briefly, this system worked as intended within limitations imposed by speed and dynamic range of the magnetometer/computer system, control authority, aliasing, and software accuracy. We then became aware of a modification to the position detectors which simply avoided most of the remaining difficulties with the controller and subtraction system.

The modification to the position detector circuit originated with E. Maypoles, H. J. Paik and K. Y. Wang [4], and was used with some degree of success by H. A. Chan in a gravity gradiometer at the University of Maryland [5]. Basically, the new circuit combines two of the old circuits to perform a precision differential measurement, and takes over some of the control functions as well.

Figures 5.a and 5.b show the position detector circuit for one mass. The two loops of the circuit contain trapped fluxes Φ_a and Φ_b, which give rise to persistent currents I_1, I_2, and I_3 in the corresponding inductances Li. The test mass M is suspended between L_1 and L_3, while L_2 is coupled to a SQUID magnetometer which measures the flux due to I_3. Both L_1 and L_3 are changed by the presence of the superconducting mass. Because the flux is constant in any superconducting circuit, the currents must change to balance the changes in inductance. Therefore, I_2 changes in proportion to the displacement of M. Specifically,

$$I_2 = \frac{L_1\Phi b - L_3\Phi a}{L_1L_3 + L_2(L_1 + L_3)}$$

where L_1 and L_3 are functions of X, the mass position. The sensitivity of the flux Φ_s at the SQUID to a displacement of the mass is therefore

$$\frac{d\Phi_s}{dx} = KL_2 I_2 = \frac{KL_2(\Phi_a - \Phi_b)}{L_1^2 + 2L_2 L_1} \frac{dL_1}{dx}$$

where we have let $L_1 \cong L_3$ and $dL_1/dx \cong -dL_3/dx$, and K is a coupling coefficient. The SQUID gives an output proportional to Φ_s which may be used as raw displacement data or used to drive a servo loop. Observe that the sensitivity is a linear function of Φ_a and Φ_b ; that is, contours of equal sensitivity are straight lines in the (Φ_a, Φ_b) plane.

This circuit gives an exceptionally stable and sensitive position measurement. The sensitivity is continuously adjustable by changing Φ_a and Φ_b (or equivalently I_1 and I_3), being limited only by the critical current of the wire and the resolution of the SQUID. With $I_i = 1$ A , the present system can resolve less than 0.01 Angstrom.

The position readout exerts a restoring force on the test mass. The acceleration sensitivity f depends on the ratio of the position sensitivity to the amplitude of the motion caused by f , which in turn depends on the signal frequency ω and the natural frequency ω_o of the mass [6]. An optimum value for I_i occurs when the forces from the readout and any residual forces from the bearing are approximately equal in magnitude; but at the precision we are aiming for, there is a large enough margin of sensitivity, and a sufficient amount of noise, that it is better to use the readout restoring forces to match the natural frequencies of the two test masses in their respective bearings. If we adjust the periods of the test masses to be identical, the masses will respond to an external disturbance with the same displacement as a function of time, and their differential mode will not be excited. This makes possible very sensitive differential acceleration measurements in the presence of external noise. In addition to period matching, it is important that the damping times of the test masses match fairly well to get a good common mode rejection ratio; fortunately, if the quality factor of the test mass oscillations is Q , the damping times need to match only to within Q times the matching of the periods.

The readout forces produce an effective spring constant

$$\frac{dF}{dx} = -\frac{1}{2(L_1 L_3 + L_2(L_1 + L_3)} \left\{ \frac{d^2 L_1}{dx^2} \Phi_b^2 + \frac{d^2 L_3}{dx^2} \Phi_a^2 \right\} .$$

For reasonable component values and fluxes, this offers a wide range of periods for the test masses. What is important here is that the spring constant (or period) depends on a combination of the squares of the trapped fluxes, whereas the sensitivity depends on a linear combination. The contours of equal spring constant are ellipses in the (Φ_a, Φ_b) plane. Thus for any given sensitivity there is a range of periods available, and vice versa.

The modified circuit is shown in figure 5.c. The modification consists of joining two circuits such as figure 5.b with L_2 in common. The full solution of this circuit is algebraically complex and not particularly enlightening, and will not be presented here. In use, the position sensitivities of the circuits for M_1 and M_2 are adjusted to be equal and opposite. The current in L_2 then depends only on the difference in the test mass positions.

Next, the mass periods are chosen to be equal using the remaining freedom in the setup, so that the differential mode is insensitive to vibrational noise. The limitation to the sensitivity of the system is common mode rejection and cross-coupling from other normal modes of the test masses. It should be possible to adjust the periods and sensitivities to get a common mode rejection ratio of 10^5. The other normal modes of the test masses are all at least one order of magnitude higher in frequency than the sensitive mode, and the position detector has been measured to be more than three orders of magnitude less sensitive to them. There is, therefore, a reasonable expectation of achieving a sensitivity five orders of magnitude better than that allowed by vibrational noise.

The test mass positions and dynamics are now determined largely by the position detector circuit. The remaining control requirements are modest: added damping and integral control of the positions. This will reduce cross-coupling by minimizing the amplitude of residual oscillations, improve the matching of the test mass dynamics, and guarantee that the equilibrium positions do not shift.

4. Development of the laboratory instrument.

During the period of this contract we have continued development of a ground-based version of the equivalence principle experiment, funded partly by NASA and partly by NSF. The NASA portion of the experiment concerns technology development and performance tests using the laboratory instrument as a test-bed for ideas related to the orbital equivalence principle experiment. We found a number of important results and made some very significant innovations and improvements during the period of funding.

The most significant results from the laboratory were:

* Development of an air bearing pendulum vibration isolation system.
* Increasing automation and precision of the experiment.
* Testing and development of two generations of magnetic bearings.
* Apparent detection of the gravitational field of a laboratory mass.
* Identification and solution of a serious magnetometer problem.
* First equivalence principle data.
* Stability tests.
* Identification of the major source of residual forces on a test mass.

Further extremely significant progress has been made under our new contract. This is reported in the first status letter for NAG8-026 for August-October 1984 [Appendix 1]. We will now discuss these topics in order.

The first significant achievement came after moving into a new laboratory. This was successful testing of an antivibration stand which imitates the motion of a 200 meter long pendulum, using an air bearing that has a curved surface. A long pendulum gives ideal isolation from horizontal vibrations; it may be thought of as being in zero gravity horizontally since all the restoring force is gravitational. Figure 6 is a photograph of the pendulum, with the equivalence principle apparatus in place, in the new lab.

FINAL REPORT ON CONTRACT NAS8-33796 "A PRELIMINARY STUDY OF A CRYOGENIC EQUIVALENCE PRINCIPLE EXPERIMENT ON SHUTTLE"

I. Introduction

This report summarizes results of preliminary studies for a cryogenic orbital equivalence principle experiment on Shuttle, which were performed during the contract period from April 30, 1980 through August 1, 1984. During this period we made significant advances in understanding the requirements for the experiment, developing technology necessary to do it, and preliminary design work.

The main areas of investigation under this contract may be broadly divided into four categories, which will be discussed in section III below:

1) Studies of the Shuttle environment, including interference with the experiment, interfacing to the experiment, and possible alternatives.

2) Numerical simulations of the proposed experiment, including analytic solutions for special cases of the mass motion and preliminary estimates of sensitivity and time required.

3) Error analysis of several noise sources such as thermal distortion, gas and radiation pressure effects, and mechanical distortion.

4) Development and performance tests of a laboratory version of the instrument, supported partly by this contract and partly by NSF.

II. Background and Experiment Description

The Weak Equivalence Principle is the hypothesis that all test bodies fall with the same acceleration in the same gravitational field, and this principle is the experimental foundation on which the geometrization of space-time in Einstein's General Theory of Relativity is built. The central place of this principle in Einstein's and other metric theories of gravity emphasizes the importance of testing it to the best possible accuracy. Any failure of the universality of free fall would necessitate a theoretical revolution.

The current limit on violations of the Weak Equivalence Principle, measured by the ratio of the difference in acceleration of two test masses to their average acceleration, is about 3 parts in 10^{11} [1]. We anticipate that this can be improved in a Shuttle experiment to a part in 10^{15}, and in a drag-free satellite to about a part in 10^{17}.

Conceptually, the experiment for which this work was performed is similar to Galileo's purported experiment of dropping different weights from the Leaning Tower of Pisa, except that instead of two balls dropping a few tens of meters and striking the ground, two concentric bodies of different materials are placed in a satellite and fall all the way around the Earth. The bodies are a short rod and a cylinder kept oriented in inertial space and constrained to relative motion in one dimension by magnetic bearings. Figure 1 shows a conceptual view of the two masses. As they orbit the Earth, they are subjected simultaneously to the centrifugal acceleration of the orbital motion and the gravitational pull of the Earth. If the ratios of gravitational mass to inertial mass of the two bodies are different, they will have

The air bearing pendulum does not behave perfectly because of turbulence in the gas film; but it does provide 30 db of isolation from horizontal motions in the range from 50 Hz to as low as we can measure (< 0.1 Hz) (Fig. 7). We have never completed the full three dimensional isolation as intended because of lack of manpower and more urgent concerns with the experiment. Development of this system is resuming now that the more important technical problems with the experiment are under control.

We have gradually increased the degree of automation of the experiment to the point where all of the setup procedures for the position detectors, and the data input and analysis, are now done by computer. In early 1980 this was almost entirely done by hand. This has made great improvements in reliability and precision, because the computer rarely forgets an operation and has excellent timing; clearly this is important in data input, but it is also necessary for the setup process, where we found that small variations in technique and timing can lead to overheating and failure to trap the proper amount of current. Accurate and reproducible setups are essential for the period and sensitivity matching of the differential accelerometer. We got 16 bit A/D converters for the SQUID magnetometers in 1981, and later extended the useful range of the magnetometers to about 7 orders of magnitude by a flux-counting technique. This is also essential for the experiment.

We have gone through two generations of magnetic bearing during the funding period. In 1980 we had only the first generation bearings from the original apparatus, which had been shown to be magnetically contaminated although they were mechanically very smooth. These had been used to show feasibility and confirm their theory of operation by measuring the resonant frequencies of the test masses levitated in them, and continued to be used through the first equivalence principle measurements in 1982. We started the completely non-magnetic and mostly non-conducting second generation bearings in 1981 but did not start performance tests on them until early 1983. They had significantly different characteristics from the first generation bearings. Unlike in the first bearings, the period of the test mass was almost independent of position, although not much longer than in the older bearings. These bearings showed a serious tendency to crack on thermal cycling, which was a main reason for retaining the old bearings through 1982, and which slowed development. In spite of the cracking, we were able to show that the residual period was independent of the weight of the test mass used and not due to electric charging of the mass, but did not understand the reason for this until late 1983.

As of May 1983, it became apparent that the second generation bearings had a flawed design that caused the cracking problem. We developed and tested the third generation bearings in less than two months. These bearings use superconducting wires stretched like guitar strings over a substrate, and are very robust. They are held together by thermal contraction instead of being torn apart by it; and even better, they take only three days to make as compared with a month or more for the earlier versions. The third generation bearings act like the second generation bearings did before they cracked: the period of the test masses was unexpectedly short (about 2 seconds) and nearly independent of position. At least a ten second period is needed to do the ground-based experiment. The sensitivity of the apparatus is proportional to the square of the period, in the absence of noise.

We did a number of tests in the next few months to determine the cause of the short periods. The first hypothesis, that the wires were sagging under the weight of the test mass, was eliminated after measuring the tension in the wires. It turned out that the extra force had its origin in the edge effect field of the magnetic bearing. This is discussed below.

One of the reasons for continuing the use of the original magnetically contaminated bearing structure was to measure its sensitivity in something resembling the intended experiment. This would make a nice demonstration of feasibility and also advance the system's development. In late 1981 we suspended 500 pounds of lead from the ceiling as a pendulum, with the intent of measuring its gravitational signal. We found a clear signal with the right amplicude after time averaging for several hundred cycles, and eventually were able to show that it could not be due to magnetic coupling from the pendulum. The signal had a large second harmonic component, however, which was likely due to the twice per cycle tug of the pendulum on the ceiling. This led to speculation that the entire signal was mechanical distortion of the building rather than gravitational. The vertical pendulum was replaced by a torsion pendulum which took no significant force to turn, and the measurement repeated. This led to a curious result: there was no reliable signal from the torsion pendulum. This led to the identification of a serious magnetometer problem.

It turned out that the magnetometers had been designed with only first-order feedback; they therefore could only track signals with a limited slew rate, and lost lock if the signals were changing too rapidly. Furthermore, because the magnetometers were almost identical and were looking at similar signals, their outputs resembled each other in the short term but were in the long run uncorrelated. The problem was exacerbated by aliasing and averaging by the computer and flux counting system. At high data rates such as were used to make the measurements with the vertical pendulum, loss of lock occurred rarely during one cycle and contributed little to the noise. At low data rates, used with the slower torsion pendulum, the loss of lock was the dominant feature.

We completely redesigned the magnetometer feedback circuits, using a second-order design that can track any constant flux rate but may lose lock on large accelerations. We also found it necessary to correct some internal circuit problems which greatly contributed to the probability of the magnetometers losing lock. After several months of work we reduced the magnetometer problem to no more than a few flux jumps per day. Many of these seem to be due to external electrical noise, but since the remaining jumps can be detected in analysis and removed, we postponed further improvement.

In the last half of 1982, after the magnetometers were fixed, we were able to take preliminary equivalence principle data, in a mode of operation resembling the original intent. A sample of the data is shown in figure 8. Trace 1 is the position of the outer test mass during the night of 7/5-6/1982. The overall mass motion is due to a tilt of about one arc-second from various causes, principally ground motion and thermal distortion of the dewar stand. Trace 2 is the difference between the inner and outer masses (after removal of 17 flux jumps). This particular trace shows that the accelerations of the masses did not differ by more than about 5×10^{-7} cm/sec^2 during the day. That is, however, not the differential acceleration sensitivity but the common

mode sensitivity. It was impossible to control the periods of the test masses in the old bearings because of insufficient control authority, and only added damping was used in this experiment. Therefore, the mismatch of the masses' dynamics caused the breadth of trace 2.

Significant results from this run included:

a. Improvement of the magnetometers to be able to follow signals of about 300,000 flux quanta at a rate of 24,000 flux quanta per second or more, with very few flux jumps.

b. The common mode sensitivity of the system was about 10^{-7} cm/sec^2, limited by seismic noise in the range 0.1 to 10 Hz. The differential sensitivity could not be measured because of limitations on the controllers.

c. Several control laws were tried successfully but because of insufficient control authority to overcome the large forces from the imperfect magnetic bearings, it was not feasible to match the periods of the test masses.

d. Integer overflow in the computer software was a problem in generating the control laws at moderate to high sensitivity, as was aliasing from higher frequency modes of the test masses. Furthermore, the computer was operating at its maximum capacity to keep up with counting flux quanta, inputting and recording data, and generating the control laws.

As a result of this run and after discussions with colleagues, it became clear that the best way to proceed would be with the superconducting position detector and differencing circuit of reference 4. The next few months were spent in analyzing the application of this circuit to the experiment, with very favorable results.

At several times during the funding period, we performed stability and noise tests of the bearings and position detector circuits. The most recent tests are the most significant. We have observed no mass sagging in the bearings provided the levitation current is below a critical value, beyond which the supercurrents are unstable. We have measured the stability of the position detectors by trapping a supercurrent of 160 mA in them and observing changes with the test mass not levitated. This current gives a sensitivity of about 1 Å per flux quantum, and although we found several anomalies (such as an abrupt increase in noise level, and a flux jump obviously caused by turning on the room lights), the total drift in a 16 hour period was 1/50 Φ_0. This is about the spread in high frequency noise. The temperature stability of the dewar environment (which is not regulated) is 20 to 40 milliKelvin per day. This is consistent with atmospheric pressure changes. There was no correlation of the temperature changes with the position monitor data. We have known for some time that there are correlations of the mass equilibrium position with atmospheric pressure and ground tilt.

The most important discovery of 1983 and 1984 was the cause of the short periods of the test masses. Because the magnetic bearings for the Earth-based experiment are half-cylinders, they have an edge effect field due to their net dipole moment. This is similar to the field that would be produced by a

current of about one-half that in the bearing, running around the perimeter of the bearing. This amounts to some 15 gauss . This stray field was known to exist from the start, but had been overlooked in later analysis.

Because the test masses are superconducting, they exclude the stray field from their volume and develop a large induced dipole moment. The dipole moment in turn interacts with the position detector coils and any other stray magnetic fields to produce the anomalous forces on the test mass. Because the field used to lift the mass is proportional to its weight, the periods produced by this effect were independent of the mass of the test mass. The complicated dependence of the periods on history of the run was due to small differences in the setup procedure for the position detector, which was done manually at that time. When these procedures were automated, the behavior of the mass became very much more reproducible. We achieved periods in excess of 20 seconds in October 1983, by variations in the levitation and setup procedures.

Because the dipole interacts strongly with the position detector coils, it tends to couple all of the vibrational modes of the test mass into them. This explained some troublesome high frequency signals which we had been seeing for years, and also implied a way to get rid of them. We confirmed the model of the induced dipole early in 1984 by partially cancelling out the stray field with a compensation coil around the perimeter of the bearing. The result is shown in figure 9. We have now developed a self-cancelling winding scheme for the half-cylinder bearings.

The bearings for the orbital experiment will be full cylinders, and will not have this particular effect. However, there are also end effects due to the finite length of the bearings, and we will have to take account of them. The expectation is that this will not be a serious problem.

IV. Summary and Status

These results have important and favorable consequences for the Orbital Equivalence Principle Experiment on Shuttle. The various studies we have made on the shuttle environment, error analysis, systems analysis, and performance tests with the laboratory experiment show significant progress during the period of this contract. Since receiving our new contract (NAG8-026), we have resolved the forces on the test mass into three clearly separable components, one of which is the dipole force above. We have also solved several long-standing technical problems, including production of perfectly superconducting joints and measurement of superconducting circuit parameters in place in the apparatus. These methods are absolutely essential for the orbital experiment. We hope to be able to complete the ground-based equivalence principle experiment within a year. Our plan for the orbital experiment is to bring it to the stage of Conceptual Design Review within approximately six to nine months.

References

1. Roll, P. G., Krotkov, R., Dicke, R. H., "The Equivalence of Inertial and Passive Gravitational Mass", Annals of Physics 26, 442-517 (1964). Since this measurement, V. B. Braginski has claimed a measurement to one part in 10^{12}, and Keiser and Faller have performed an experiment to a few parts in 10^{10}.

2. Kullas, M. C., Handbook on Astronaut Crew Motion Disturbances for Control System Design, NASA Reference Publication 1025, May 1979.

3. Ray, J. C., private communication; TIP-III DISCOS STUDY GROUP REPORT, Johns Hopkins University-Applied Physics Laboratory, JHU/APL February 1980, SDO-5592.

4. Maypoles, E., Paik, H. J., and Wang, K. Y., "Superconducting Gravity Gradiometers", Future Trends in Superconducting Electronics (Charlottesville, 1978), p. 166.

5. Chan, H. A., "Null Test of the Gravitational Inverse Square Law with a Superconducting Gravity Gradiometer", Ph.D. Thesis, University of Maryland, College Park, MD (July 1982).

6. Worden, P. W. Jr., and Everitt, C. W. F., "Tests of the Equivalence of Gravitational and Inertial Mass based on Cryogenic Techniques", Experimental Gravitation, B. Bertotti (ed.) (Academic Press, N.Y. 1973).

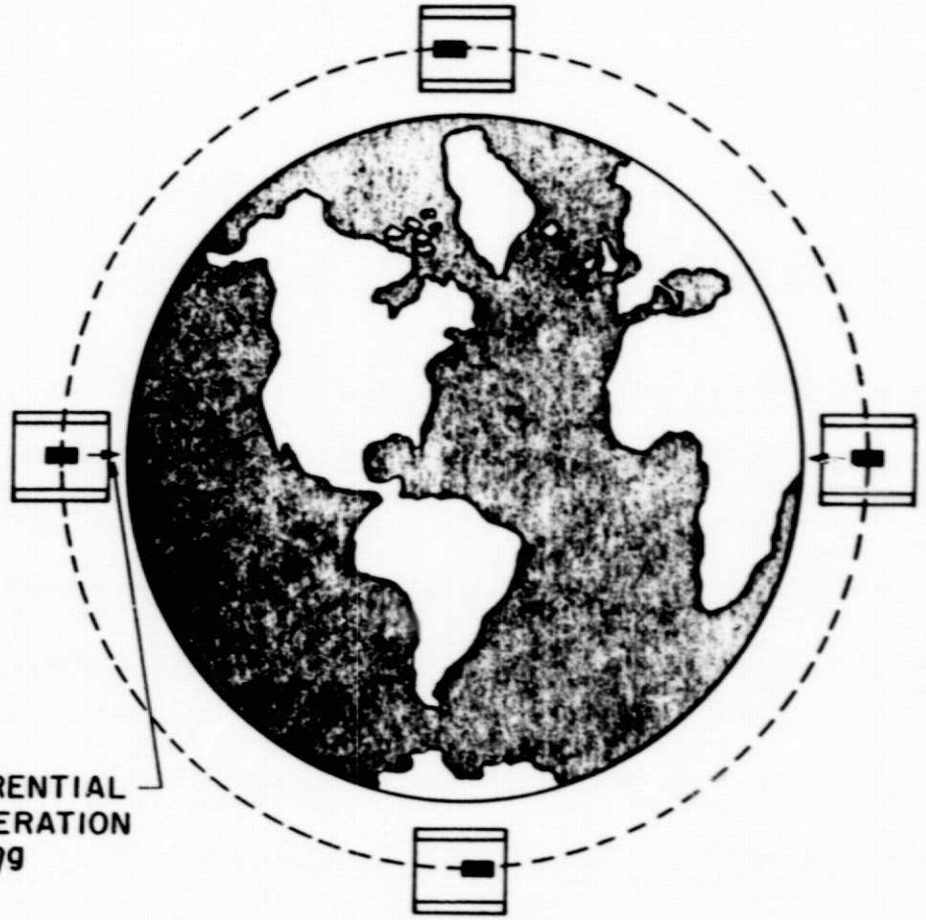

Figure 1

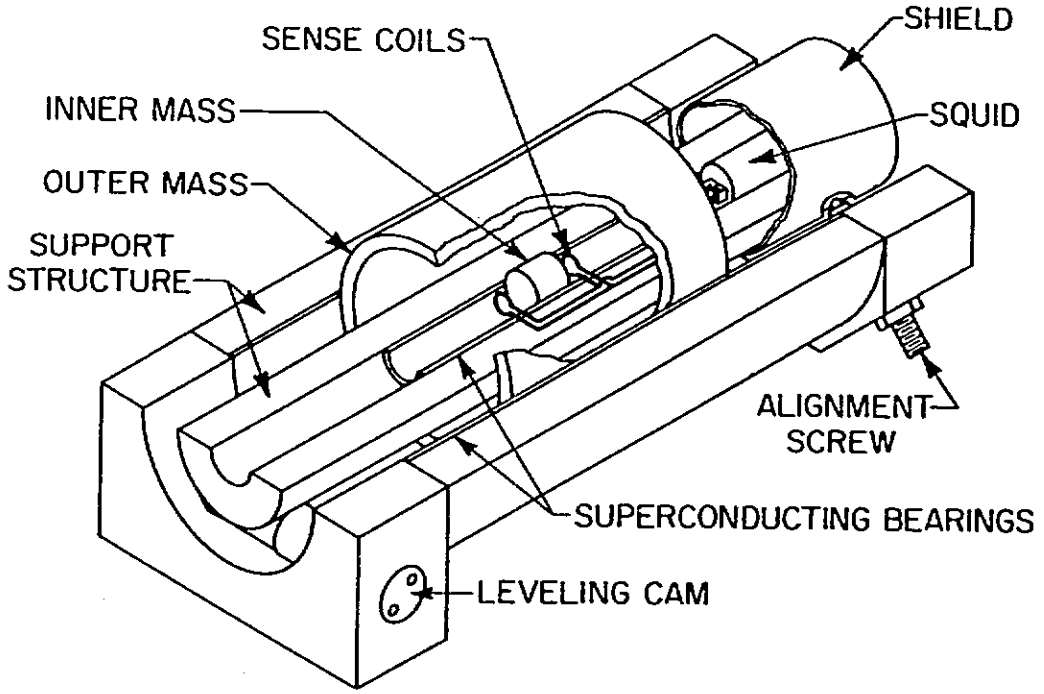

EQUIVALENCE PRINCIPLE ACCELEROMETER

Figure 2

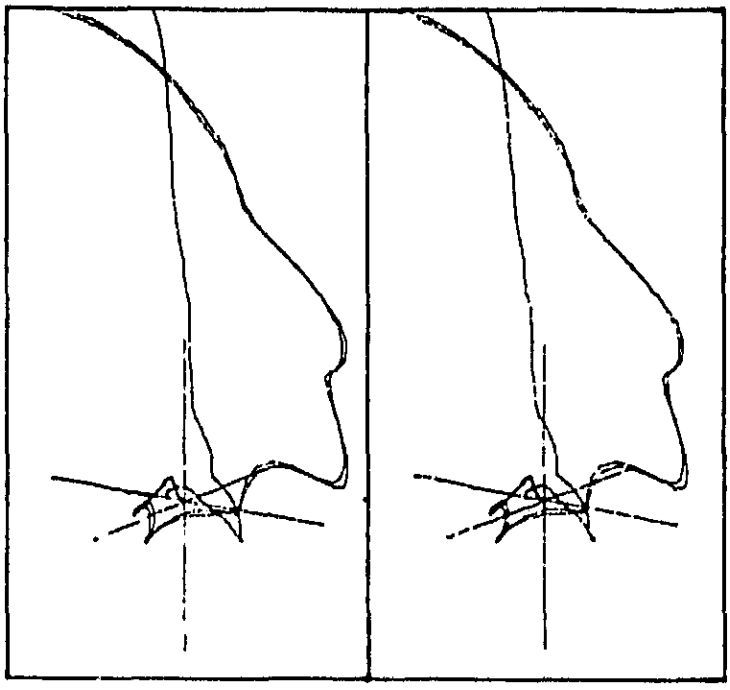

Fig. 3.a Equivalence Principle Simulation. Two test masses were started from rest at $(x,y,z) = (0,0,0)$ and $(0,0.01,0)$ cm, while the shuttle C.G. started from $(0,1,0)$ cm. The identical masses are constrained to be near the x-axis in the shuttle frame by a 15-second spring constant. The shuttle is excited by 10^{-4}g white noise in a $\frac{1}{2}$-Hz bandwidth. This stereo view is from a frame co-orbiting with the initial conditions of the mass at the origin.

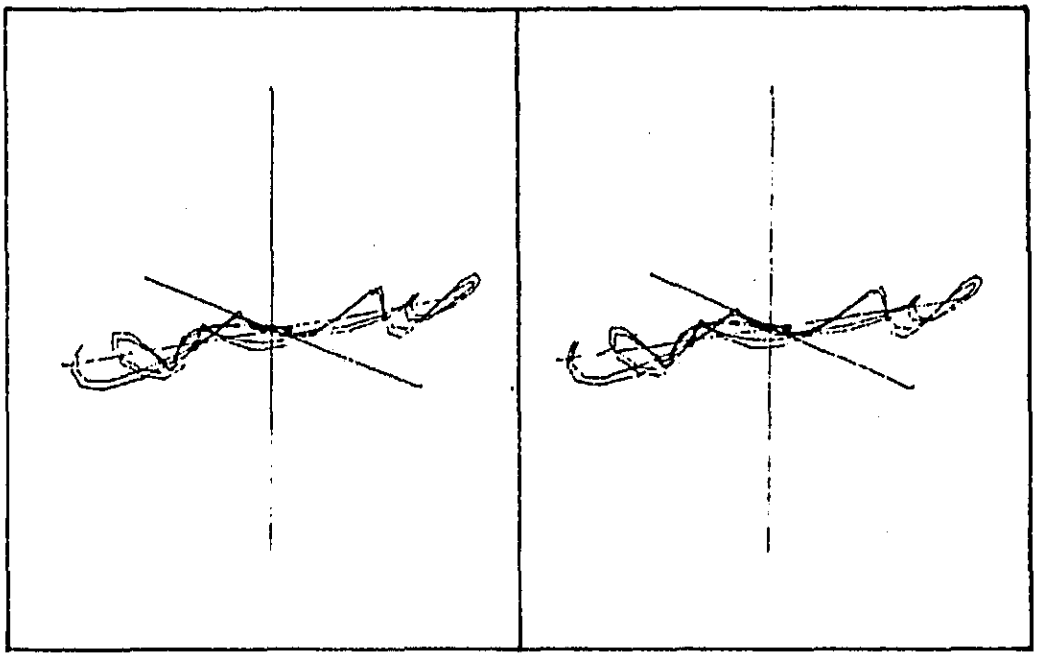

Fig. 3.b The same data as Fig. 3.a viewed from the shuttle frame. The segment of data here covers about two minutes of real time. The coordinate axes in both figures are 10 cm long.

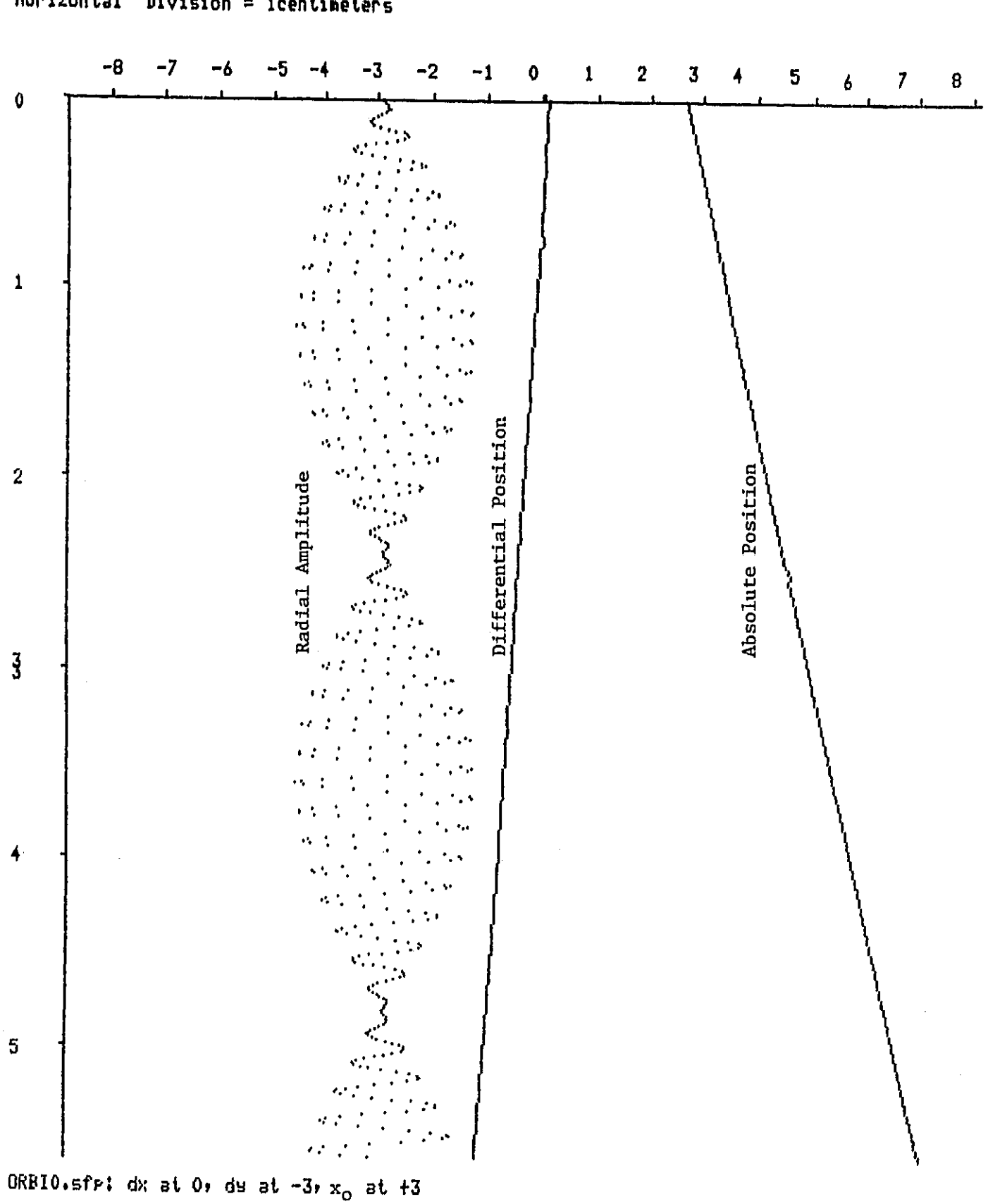
Vertical Division = 100seconds
Horizontal Division = 1centimeters
-8 -7 -6 -5 -4 -3 -2 -1 0 1 2 3 4 5 6 7 8
0
1
2
3
4
5
Radial Amplitude
Differential Position
Absolute Position
ORBIO.sfp: dx at 0, dy at -3, x_o at +3

Figure 4

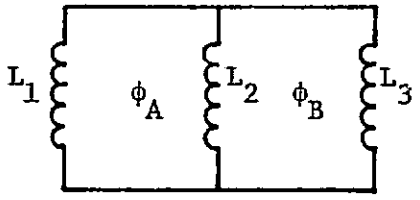

Figure 5a

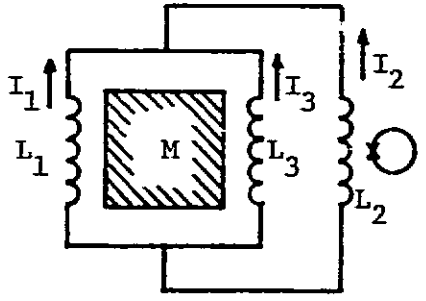

Figure 5b

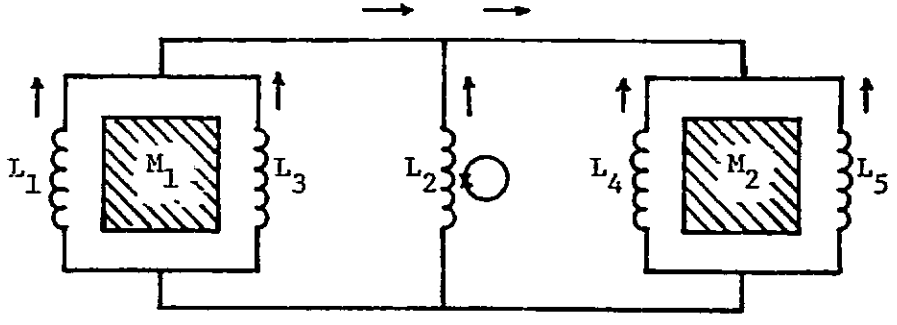

Figure 5c

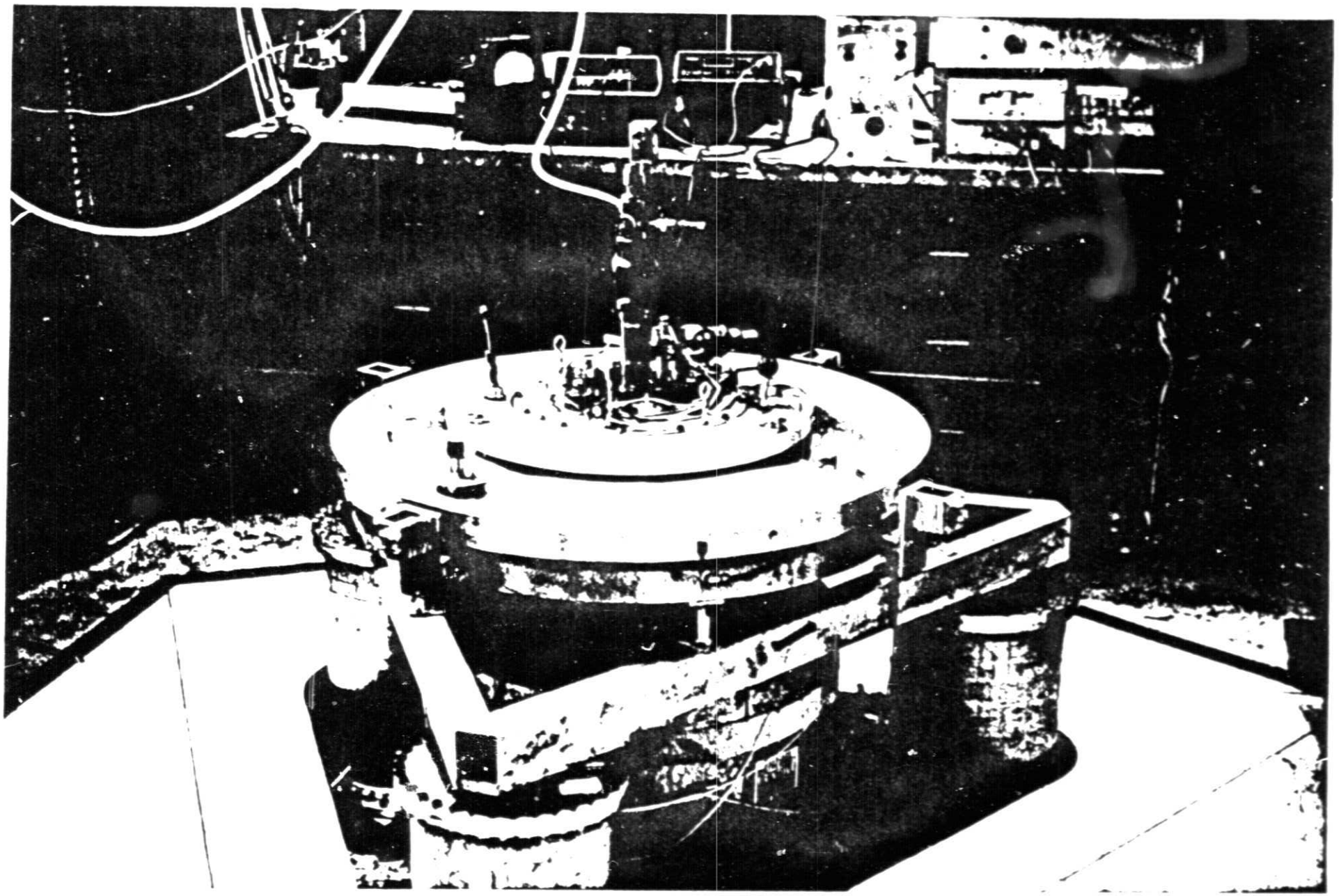

Figure 6: Laboratory version of Equivalence Principle Accelerometer mounted on Anti-Vibration Stand

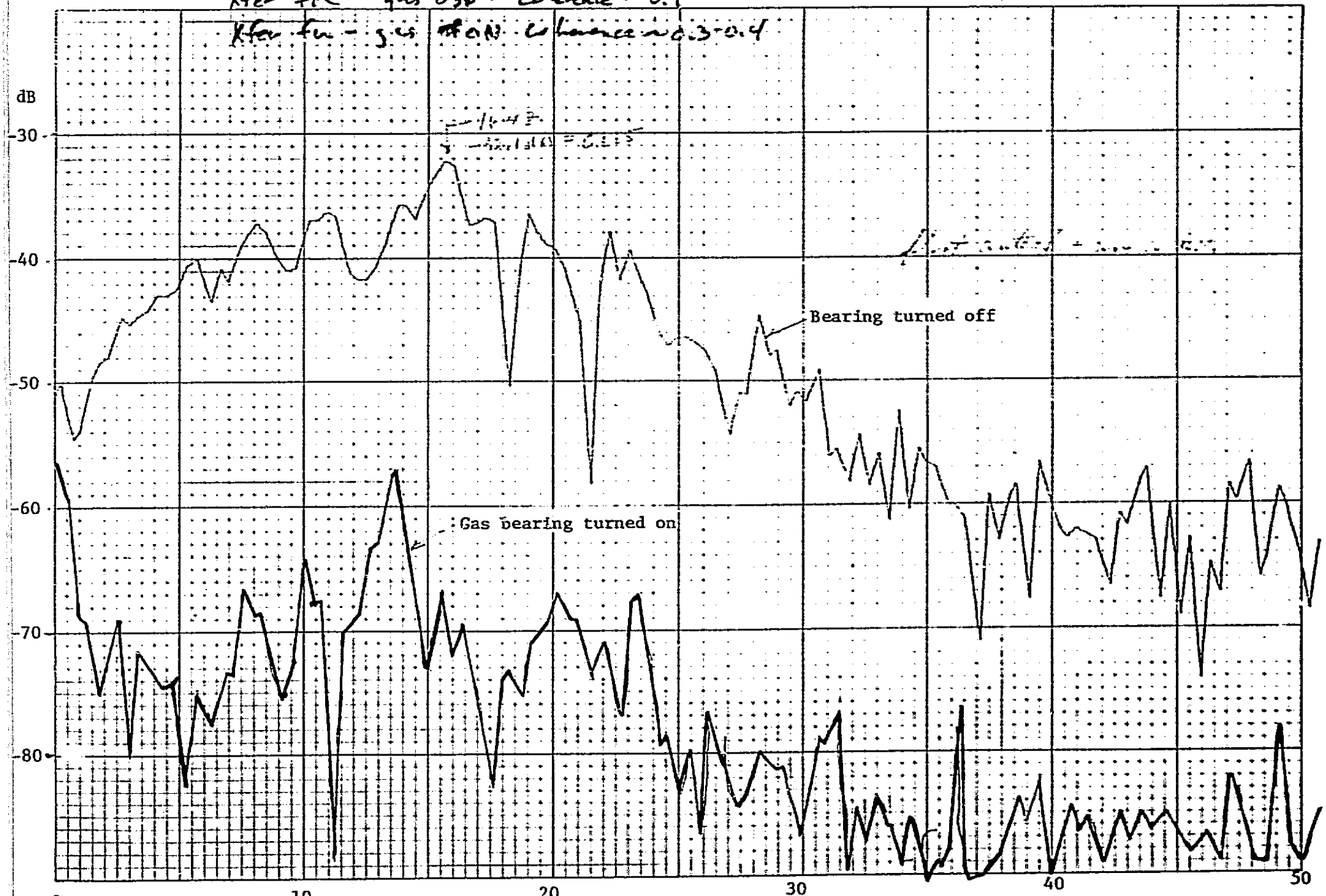

Figure 7

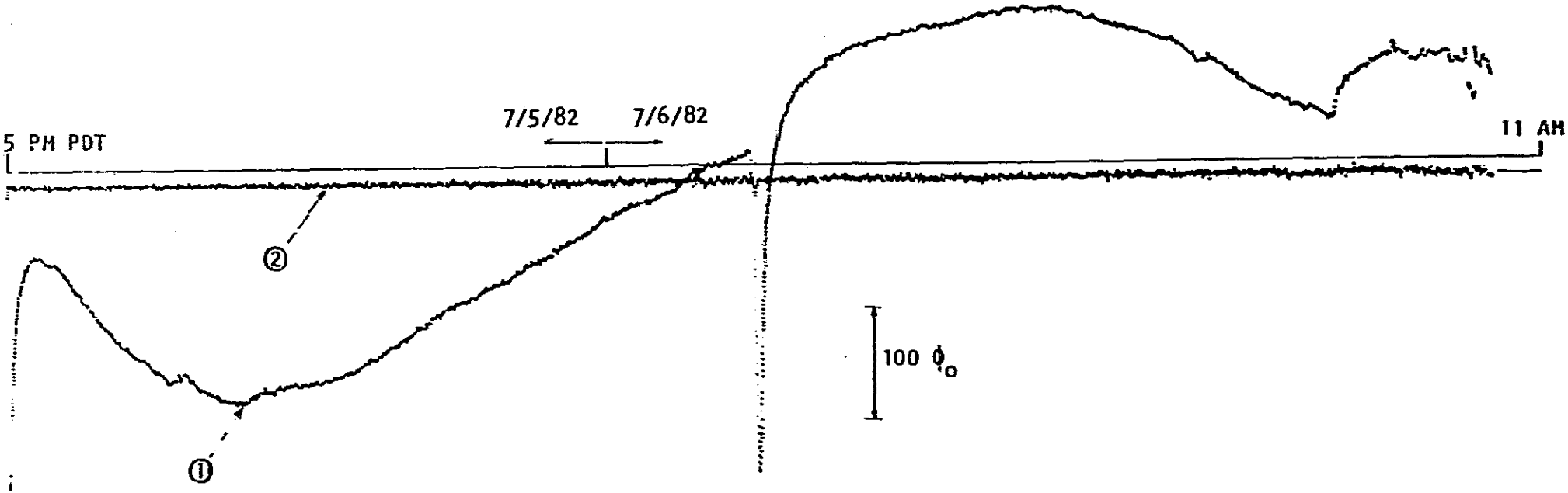

Fig. 8: EQUIVALENCE PRINCIPLE DATA
"EX70682. DAT"

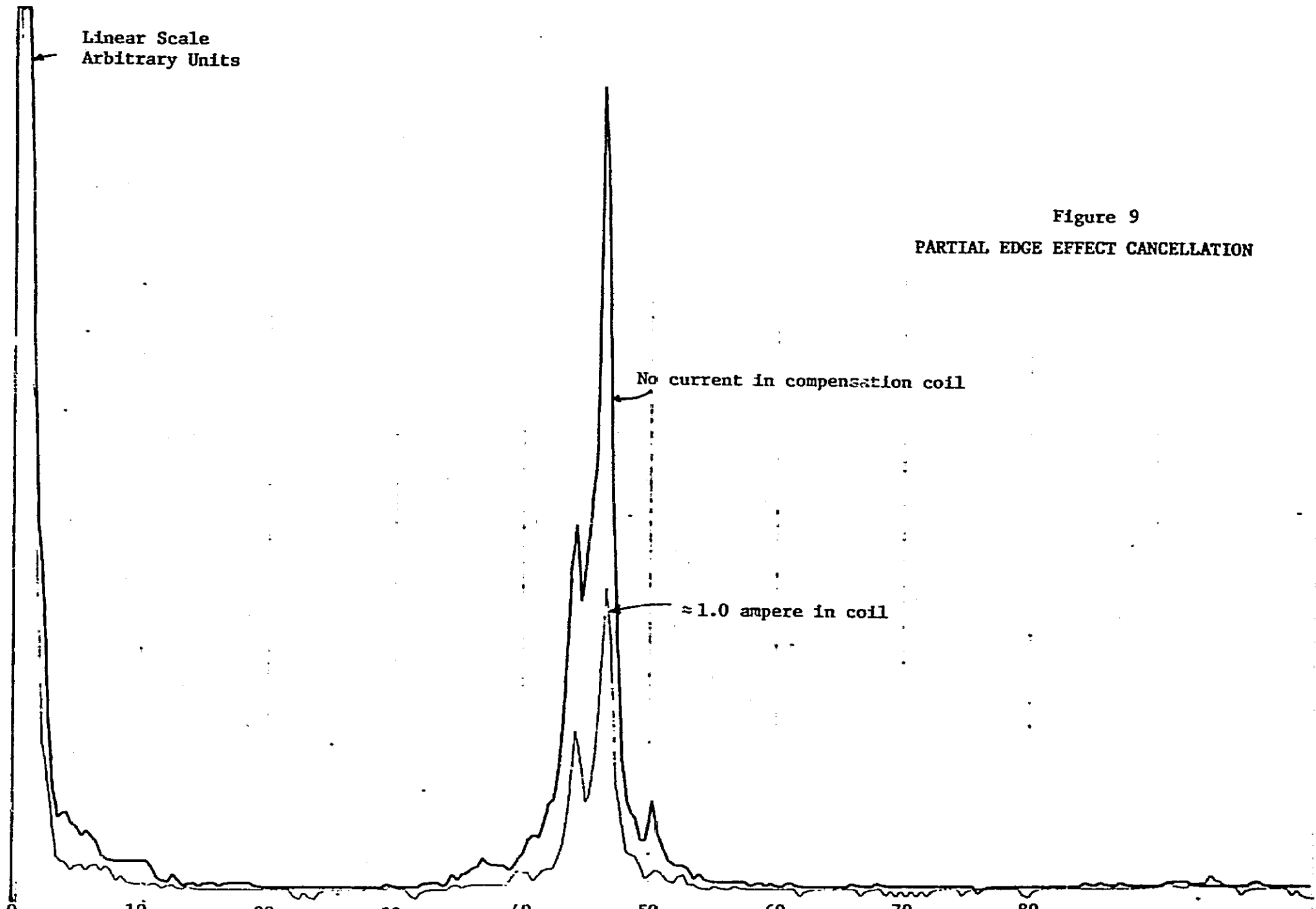

Figure 9

PARTIAL EDGE EFFECT CANCELLATION

W.W. HANSEN LABORATORIES OF PHYSICS
STANFORD UNIVERSITY
STANFORD, CALIFORNIA 94305-2184

Edward L. Ginzton Laboratory
High Energy Physics Laboratory

Telephone (415) 497- 0396

APPENDIX 1

Status Letter for August-October 1984, Grant No. NAG8-026, "A Preliminary Study of a Cryogenic Equivalence Principle Experiment on Shuttle" (Principal Investigator: C. W. F. Everitt; Associate Investigator: Paul W. Worden, Jr.)

I have studied several technical problems with the apparatus during this period, while waiting for the quartz pieces for the new magnetic bearing assembly. The latest estimate is that the pieces will be finished in mid-November, and I expect to need about two or three months to get the new apparatus together once they arrive. During the interval of waiting I have made extraordinary progress with the technical problems, amounting overall to one or two orders of magnitude in precision and ease of setup.

In August I began with a thorough study of an old problem, that of making perfect superconducting joints. A bit of thought convinced me that much of the problem was with accurate measurement of the critical current and the changes made by different joining techniques. I had been measuring these almost by hand, using a signal generator to repeatedly ramp up the input current to the flux transformer primary winding until a transition occurred in the secondary, and noting the current level on an oscilloscope. Re-examination of the data convinced me that this method was no more accurate than 10% and often much worse, because of variations in technique and timing. These variations resulted in differences in heating and trapped flux that directly affected the measurements; almost equally serious was imprecise knowledge of the properties of the flux transformer at low temperature.

I developed a system for measuring the inductance, current ratio, and critical currents of the transformer at low temperature using a 1 Hz triangle input. A much higher frequency will not do because of the small, unknown and variable resistance of the heat switches in the circuit; but at 1 Hz this impedance is much greater than that of any inductance, and can be neglected. The current ratio is found by measuring the difference in inductance of the primary with the secondary superconducting and with it normal, and finding the ratio of this difference to the mutual inductance. I automated the method, and then developed a way to check it. This is to integrate the voltage across a heat switch as it goes normal; the integral is just the total trapped flux in the coil. I found that it was possible to set up a predetermined flux in the secondary and then measure it to be within 0.1% of the expected value. To achieve this accuracy it is necessary to take

account of the roughly 100 msec cooling time of the heat switch sections (because the current is ramped, it is the time the section goes superconducting that counts rather than the time the heat is turned off), the 5 msec A/D conversion delay in the computer, and an extra delay due to ohmic heating. The remaining error seems to be caused by variable cooling of the heat switch. All of these errors can be reduced by using a slower ramp, or by making the current constant just before trapping it.

Next I investigated the superconducting joints themselves rather than measurement techniques. The results were informative. Most spot-welded test joints made with the flattened wire method developed last year had critical currents Ic greater than 60 amperes, and many were 110 amperes or more, somewhat greater than the rated Ic of the superconducting wire. The joints in the apparatus are usually worse than this. The difference turned out to be due to technique; the test joints were made with a relatively precise welding head, but those in the apparatus were made manually with a set of "tweezers" because the apparatus won't fit in the spot welder. I made a set of special tweezers which provide a calibrated heavy pressure and give good results on the test joints. I made some tests of flux creep through the joints and found none in 200 seconds.

Finally I made modifications to the apparatus to make use of the new methods of flux measurement, spot-welded the bad joint in the levitation transformer, and cooled the experiment. Measurements on the levitation circuit were quite satisfactory, and gave, for example, a current ratio of 8.045 ± 0.3%. The other parts of the apparatus gave confusing results. The mass apparently was rubbing something right in the middle of the bearing, and it was impossible to trap any current in the magnetometer position detector circuit. I used the remainder of the run for a general cleanup of electrical noise sources which interfere with the SQUID. This included a very effective filter and shield on the CRT computer terminal and RF grounding of all dewar inputs to eliminate common mode pickup in the SQUID RF circuit. There remains some work to be done on this subject, but most of the sensitivity of the probe has been eliminated and it is now possible to connect almost anything to it without seriously disturbing the SQUID. In particular it is now possible to use the photodetector and SQUID position detectors simultaneously, which was previously impossible because of a few microvolts of RF from the chopper stabilized amplifier used in the photodetector.

After warming up, I found that the source of rubbing was the light emitting diode used in the photodetector. It had slipped about 0.01" when glued in place --enough to touch the test mass, or keep a slightly larger test mass from levitating. The position detector circuit had a wiring error which took several days to fix because of the delicate 0.002" niobium wires.

In early October, I started the latest run which has continued to the present because of its excellent results. First I automated the levitation and position detector setup procedures. This was essential to get reproducible setups without overheating the apparatus. Then I did a cross-calibration of the magnetometer position detector with the photodetector. Figures 1 through 4 illustrate this. With a current of -22 mA trapped in both coils of the position detector, the magnetometer sensitivity has the S-shaped curve shown in Figure 1. As the current is reduced to zero, this curve evolves smoothly into the C-shape in Figure 2, and

as the current is increased to about 30 ma, it goes to the reversed S-shape in Figure 3. This is not quite what is expected from theory; it should go to a vertical straight line (zero sensitivity) at zero current. Figure 4 shows a family of curves calculated from a computer model. For equal currents in the two position detector coils, all of the curves should resemble the uppermost S-shaped curve. The conclusion is that there is some stray magnetic field coupling to the position detector which leaves some flux trapped in the coils when they have zero current in them. The magnetic bearing, of course, provides such a field. I made a systematic study of the magnetometer sensitivity for differing currents I1, I2 in the two coils. The sensitivity, measured as average slope, is ideally a plane surface passing through the origin of the I1, I2 plane, with constant sensitivity contours being lines of slope -1. Contours of curvature or average second derivative--i.e., how C-shaped the sensitivity is--are of slope 1, with zero curvature passing through the origin. This is what I found, except that the surfaces do not pass through the origin but somewhat below it. I found minimal sensitivity and minimal curvature near a point I1 = 40 mA, I2 = -24 mA, where the sensitivity was an S-shape with top directly above its bottom. This is impossible without an external field of some sort. The quantitative analysis of these data is still in progress, but the preliminary conclusion is that they can be understood in terms of fields external to the position detector.

An equally important result is confirmation that the magnetometer does not lose lock except under extreme conditions of noise. Figure 1 shows some offsets due to unlocking; it has the second worst unlocking out of some three dozen data files. The dewar is shaken a lot when it is tipped to take these data. For equivalence principle operation, the limitation on sensitivity due to unlocking is normal seismic noise, not dewar tipping. I am intending nonetheless to make some further improvements to the maximum flux rate that the magnetometers can handle. It is comforting to note that although the photodetector is in some ways ideal, does not lose lock and provides a useful absolute reference, it has its own problems: 50 to 5000 times less position sensitivity, about ten times higher broadband noise relative to the signal, and a drift caused by temperature effects. As the shadow of the mass moves across the photodiode, it cools off (certainly less than 0.5 K) with a time constant of the order of 1 second and its output changes. If the mass moves quickly, the effect is hysteresis; if slowly, a nonlinearity. The only solution is to operate at low light intensity and accept a still higher noise level. When the SQUID and photodetector are operated together, the correlation between their outputs is 0.98 to 1.00.

I measured the period of the test mass for a variety of conditions, and found that it depends most strongly on the position detector setup and levitation current. In particular, for one polarity of levitation current, the center position of the test mass was stable and for the other polarity it was unstable. This is only possible if there is a permanent magnetic field involved. The induced dipole moment of the test mass can interact with a static field to produce stability or instability, depending on polarity of the levitation current. Conversely, the test mass could have a permanent moment interacting with the reversible field of the bearing.

By measuring the acceleration of the test mass at each position in the bearing, it is possible to derive the effective potential in which it is moving. This was difficult with the SQUID magnetometers because of their tendency to lose lock, but

with the photodetector it is possible to average over many trials without any position ambiguity. This was a very fruitful procedure. It turns out that the potential can be divided into three clearly separable components: one which seems not to change and may be due to the physical shape of the magnetic bearing; a second which is the force due to the modulated inductance and setup current in the position detector; and a third component which is apparently the interaction between a magnetic dipole on the test mass and the position detector currents. There is more data to take and it may turn out that there are other effects as well.

Refer to the figures. Figure 5.a shows the apparently constant potential which is present when the mass is levitated and no current is in the position detector. This potential may depend somewhat on the levitation current but I have not fully documented that it does. In general the test mass is rather strongly attracted to each end by a short-range force, and has a relatively force-free and perhaps variable region in the center. Figure 5.b shows the changed potential when 37.7 mA is trapped in both coils of the position detector. By subtracting 5.a from 5.b, the potential due to the trapped current alone can be found (Fig. 5.c). This looks like the expected potential plus a constant slope. Other setup currents give similar results but with other potentials and slopes (Fig. 6.a and 6.b). Now suppose that there is a magnetic dipole on the test mass. If the magnetic moments of the position detector coils are parallel, the mass will be attracted to one coil and repelled by the other, and the total force will be approximately independent of position, i.e., the potential due to the dipole/current interaction will have a constant slope. Conversely if the coils have opposite moments, the dipole on the mass will be either attracted to both (unstable at the center) or repelled by both (stable at the center). This is precisely what is found in Figs. 6.c and 6.d. It is possible to separate the magnetic dipole force from the modulated inductance force by reversing the current. The dipole force reverses but the modulated inductance term is the same, so the difference shows the force due to the dipole. This was done for the approximately opposite cases shown. Fig. 6.c is the difference between two measurements with parallel currents, and 6.d is the difference between two measurements with antiparallel currents. Quantitative analysis of this data is still in progress.

This is excellent confirmation of the conceptual model of the apparatus. It remains to be decided whether the dipole on the test mass is permanent or induced--as this mass is a hollow shell, it could equally likely be either, or both--and whether there are any unmodelled forces remaining. The position detector forces and sensitivities are essentially as expected, and the other effects are simply added to them. The extra dipole and magnetic bearing forces are small enough that they will not necessarily cause problems, but they do have considerable nuisance potential. I am able to consistently get test mass periods of 15 seconds near the center of the bearing, but would like to get that period over a wider range of positions. The quartz pieces and new dipole-compensating winding scheme should substantially reduce the extra forces.

Finally I have made some measurements of flux creep in the levitation circuit. This begins abruptly at an input current of 2.5 amperes to the primary coil, and is clearly due to an instability in the primary winding. This is about 25% of the rated current of the wire. The superconducting joints in the primary are rather suspect because they were made with an older technique. They will be disassembled,

rebuilt, and tested when the new apparatus is put together. There is also some flux creep in the secondary which begins at about 30 amperes; the secondary has a critical current greater than 90 amperes, which could not be measured accurately because the primary went normal first. There is no evidence for flux creep outside of the levitation circuit.

These results are extremely satisfying. The experiment seems to have reached a critical mass of techniques and equipment, and while there remains a significant amount of technical work to be done, the remaining problems are well in hand. I will be spending the next few months working on them simultaneously with building the new apparatus.

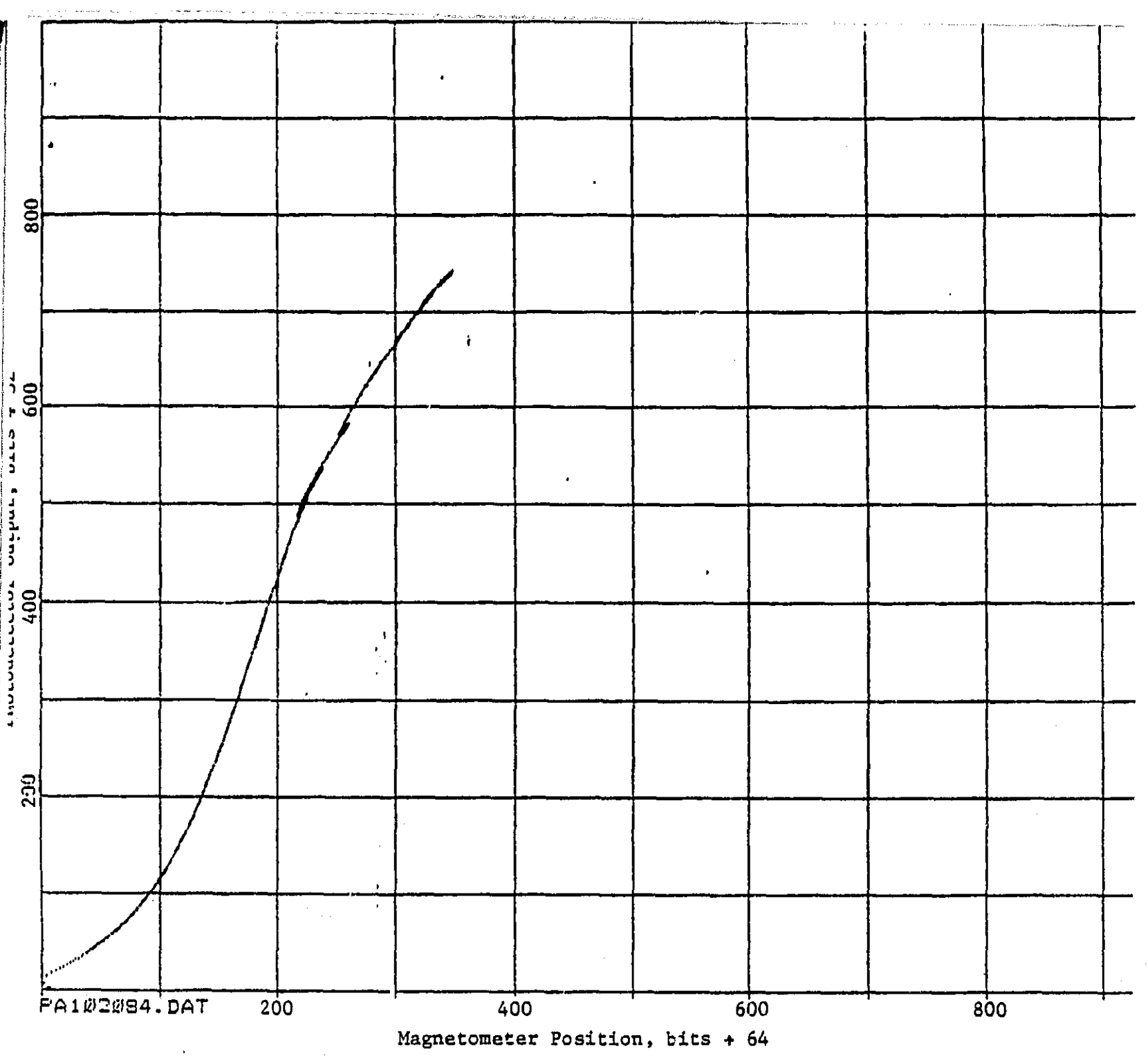

Fig. 1: Magnetometer Position versus Photodetector Position, -22 mA Setup Current

Some loss of lock occurred near magnetometer position 220.

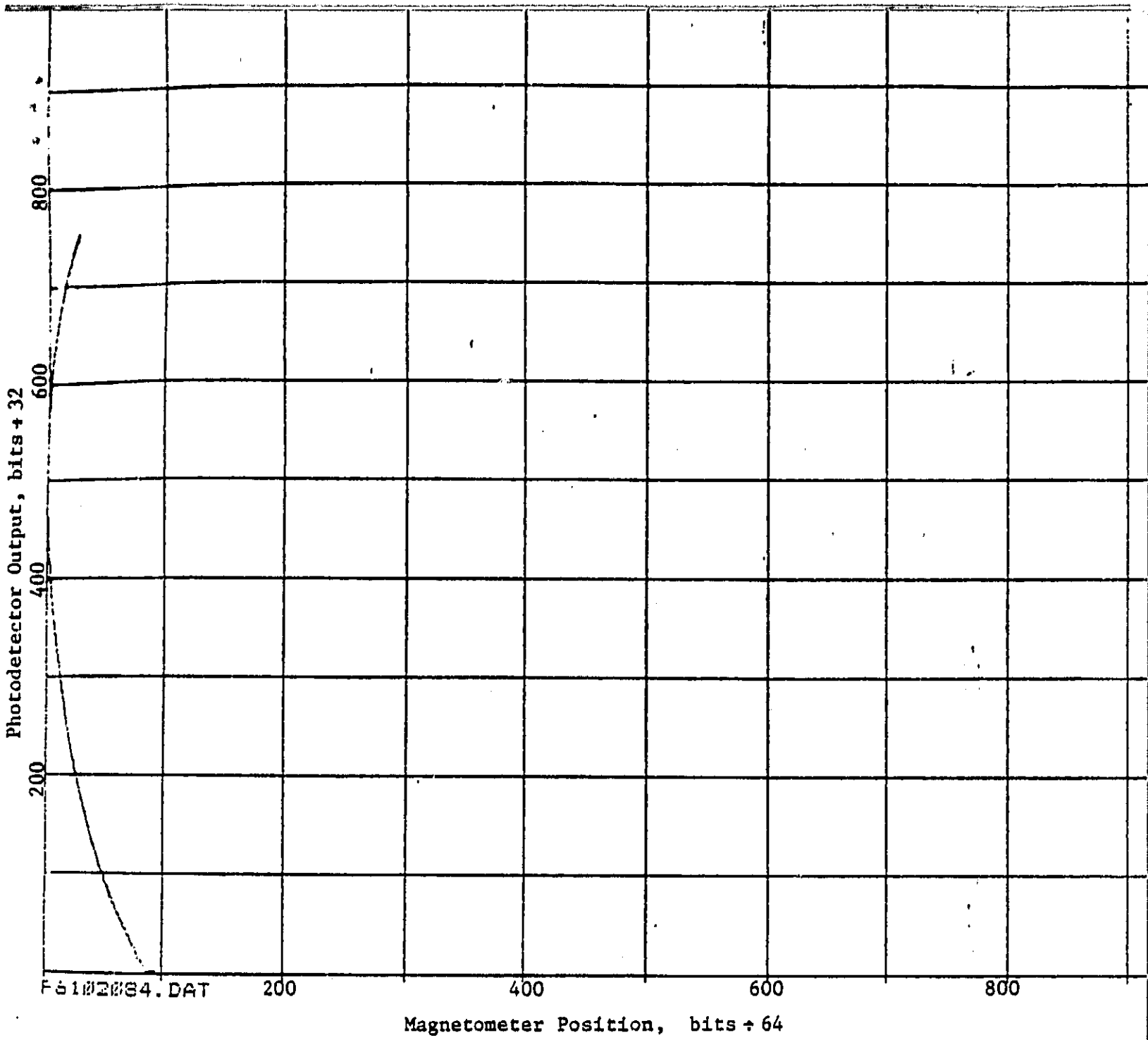

Fig. 2: Magnetometer Position versus Photodetector Position, 0.7 mA Setup Current

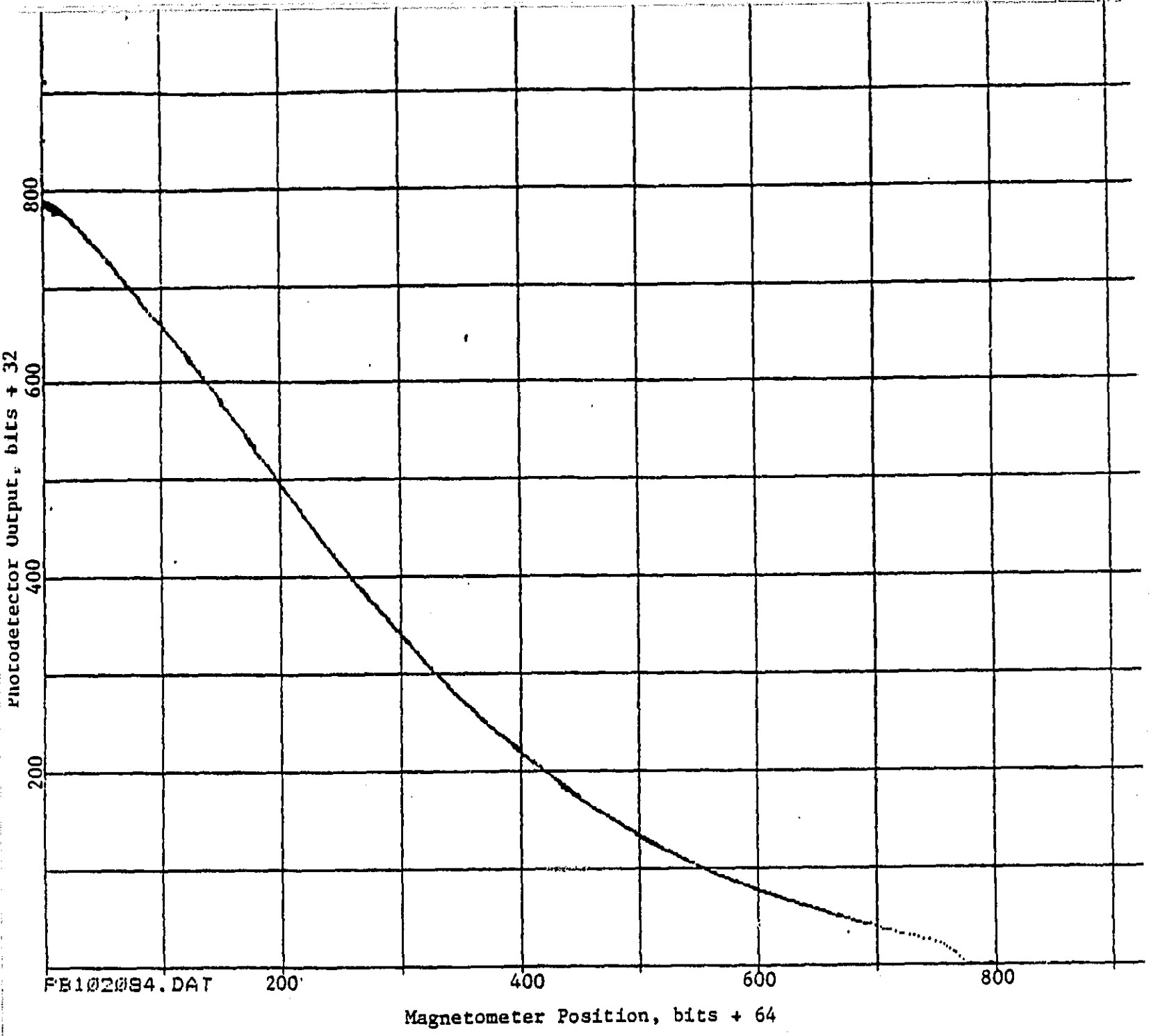

Fig. 3: Magnetometer Position versus Photodetector Position, 29.2 mA Setup Current

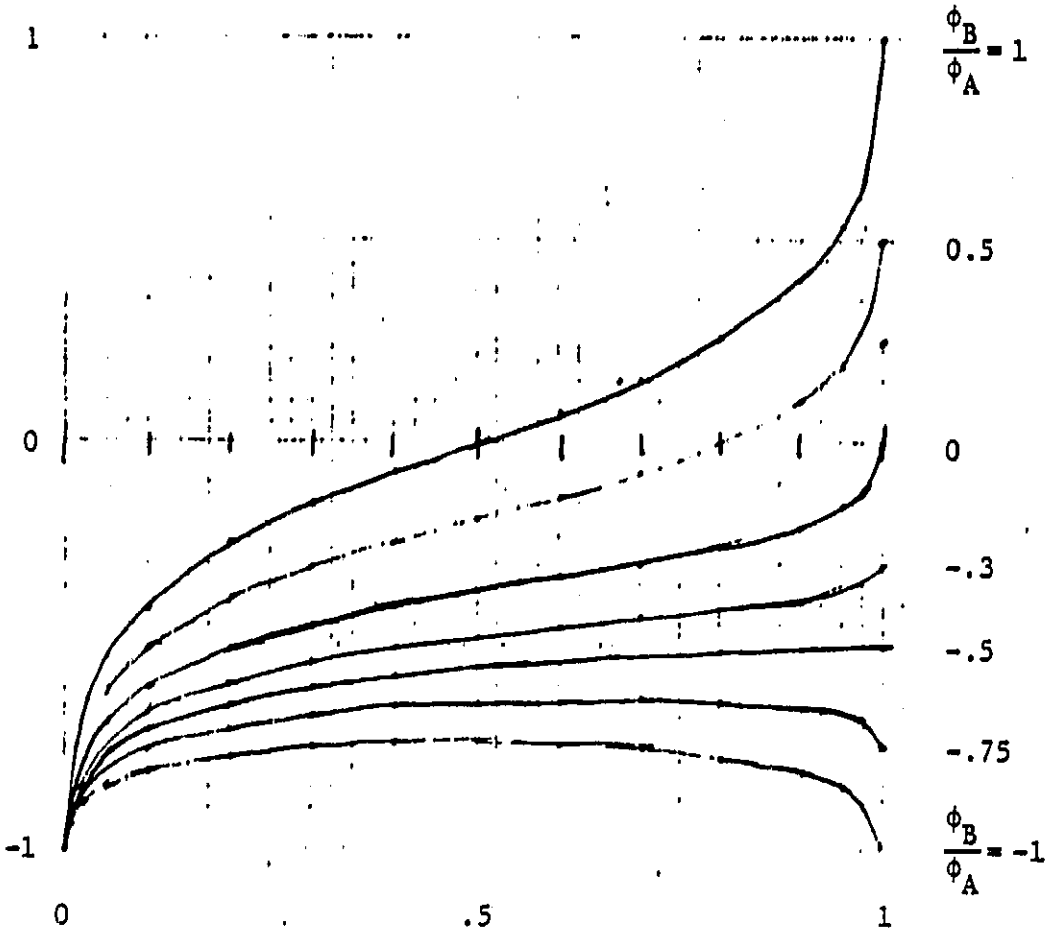

Fig. 4: Position Detector "Sensitivity" as function of flux ratio (approximate)

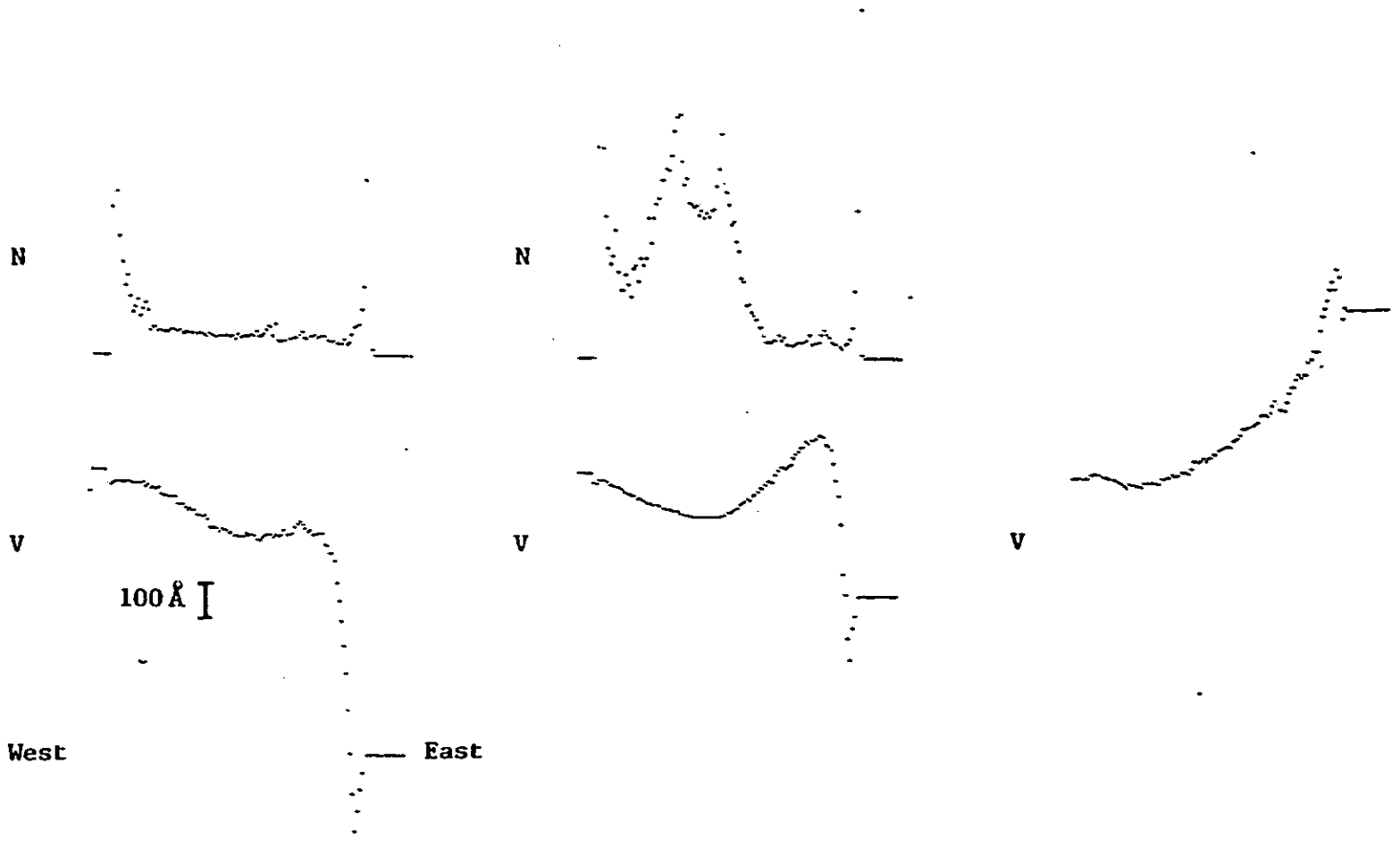

X0611.DAT

5.A

Constant Background Potential

X1611.DAT

5.B

Total Potential at
37.7 mA Setup Current

DL10611.DAT

5.C

Difference of 5.A and 5.B
Due to Setup Current Alone

Fig. 5: Effective potential on test mass. The curves labeled N show the number of data points averaged at each position. The V curves are the potential seen by the test mass at each position X. The N curves reflect the statistical error at each point, except for 4 to 6 points near the end where the potential is very uncertain. The vertical scale bar shows the potential converted to effective height in the earth's gravity according to $h = V/mg$.

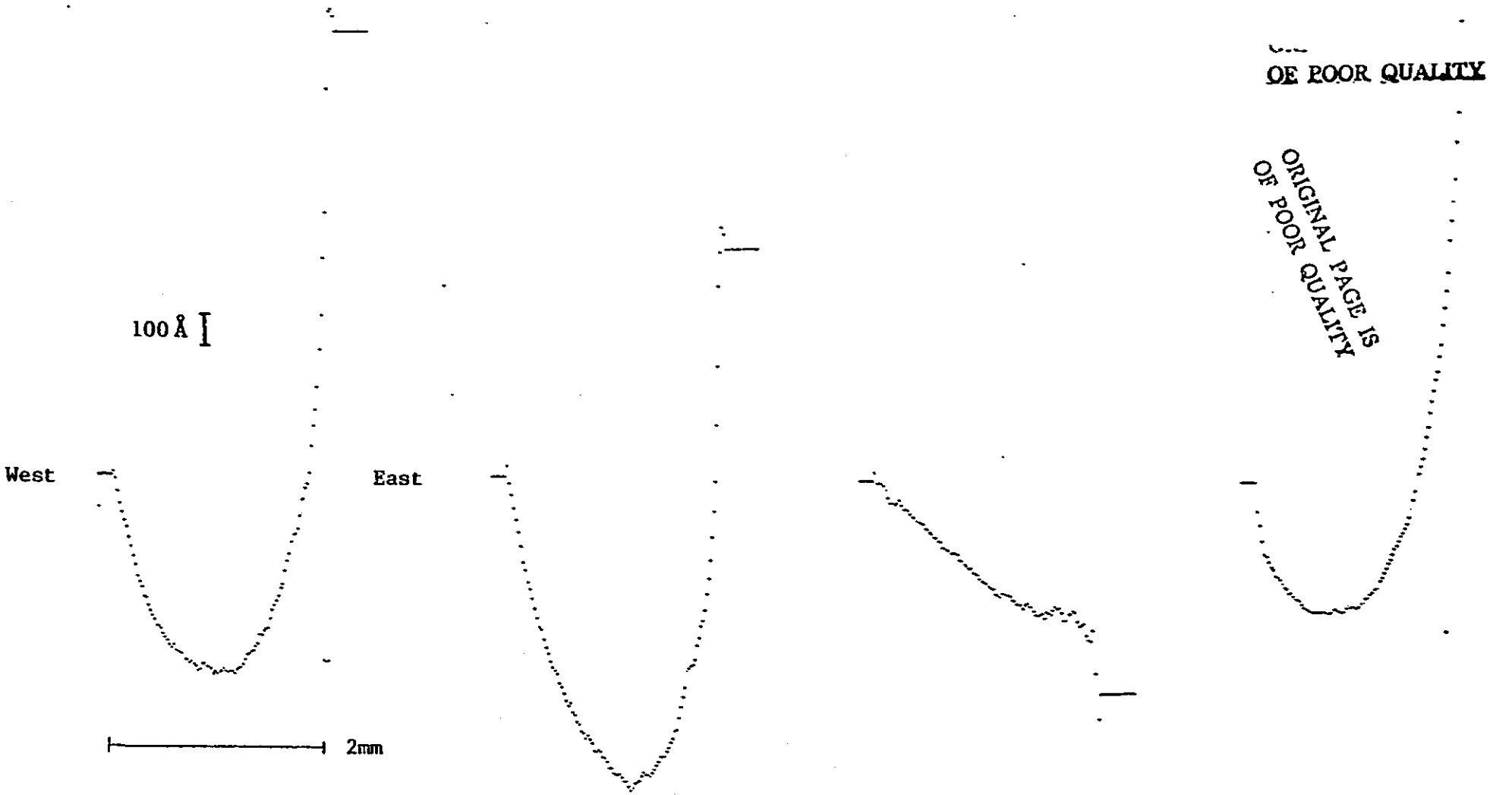

DL30611.DAT

6.a

Potential Due to
71.9 mA Setup

DL50611.DAT

6.b

Potential Due to
−64.8 mA Setup

DL53611.DAT

6.c

Difference Between 6.a and 6.b
Potential Due to Permanent
Dipole on Test Mass, Parallel Case

DL79611.DAT

6.d

Potential Due to
Dipole Anti-
parallel Case

Fig. 6: Separation of magnetic dipole potential. The 5-6 points nearest the East end are very uncertain because the mass tended to stick there, and an unknown number of points with acceleration were averaged with them.